Electronic Supplementary Material (ESI) for Physical Chemistry Chemical Physics.

Supporting Information

Cocrystals of 1,2,4-thiadiazole-based potent neuroprotector with gallic acid: solubility, thermodynamic stability relationships and formation pathways

Artem O. Surov[a], Andrei V. Churakov[b], Alexey N. Proshin[c], Xia-Lin Dai[d], Tongbu Lu[e], German L. Perlovich[a,*]

[a]Institution of the Russian Academy of Sciences, G.A. Krestov Institute of Solution Chemistry RAS, 153045 Ivanovo, Russia.

[b]Institute of General and Inorganic Chemistry RAS, Leninsky Prosp. 31,119991, Moscow, Russia.

[c]Institute of Physiologically Active Compounds of the Russian Academy of Sciences, 142432, Chernogolovka, Russia

[d]School of Pharmaceutical Sciences, Sun Yat-Sen University, 510006, Guangzhou, China

[e]Institute for New Energy Materials and Low Carbon Technologies, Tianjin University of Technology, 300384, Tianjin, China

* To whom correspondence should be addressed:

Telephone: +7-4932-533784; Fax: +7-4932- 336237; E-mail: glp@isc-ras.ru

Experimental details

1. Single-crystal X-ray diffraction structure determination of [TDZ:GA:H2O] (1:1:1)

Single-crystal X-ray diffraction data for the [**TDZ:GA:H2O**] (1:1:1) cocrystal were collected on a Bruker SMART APEX II diffractometer using graphite-monochromated Mo-*K*α radiation (λ = 0.71073 Å) at 150K. Absorption correction based on measurements of equivalent reflections was applied.[1] The structure was solved by direct methods and refined by full matrix least-squares on F^2 with anisotropic thermal parameters for all the non-hydrogen atoms.[2] All carbon H atoms were placed in calculated positions and refined using a riding model. All amino and hydroxy H atoms were found from difference Fourier synthesis and refined with restrained O-H distances. Terminal –CHMe(OH) group was found to be disordered over two positions with occupancy ratio 0.807(2)/0.193(2). Hydrogen atom H6 in gallic acid molecule was also equally disordered.

2. Solid-state DFT calculations

The DFT calculations of the [**TDZ:GA:H2O**] (1:1:1) cocrystal were performed with the CRYSTAL14[3] software suite using B3LYP functional with the Grimme[4] dispersion correction (D2) and 6-31G(d,p) basis set. The default CRYSTAL14 computation options are used to achieve an appropriate level of accuracy in evaluating the Coulomb and Hartree-Fock exchange series and the exchange-correlation contribution. Tolerance on energy controlling the self-consistent field convergence for geometry optimizations and frequencies computations is set to 1×10^{-9} and 1×10^{-10} hartree, respectively. The shrinking factor, reflecting the density of the k-points grid in the reciprocal space, was set at least to 3. In this work, the space group, unit cell parameters and positions of the heavy atoms were fixed and the structural relaxations were limited to the coordinates of the hydrogen atoms. The [**TDZ:GA:H2O**] (1:1:1) crystal structures that consisted of only one disordered component of the **TDZ** molecule (0.807 or 0.193 site occupancy) were used as the starting point in the solid-state DFT computations.

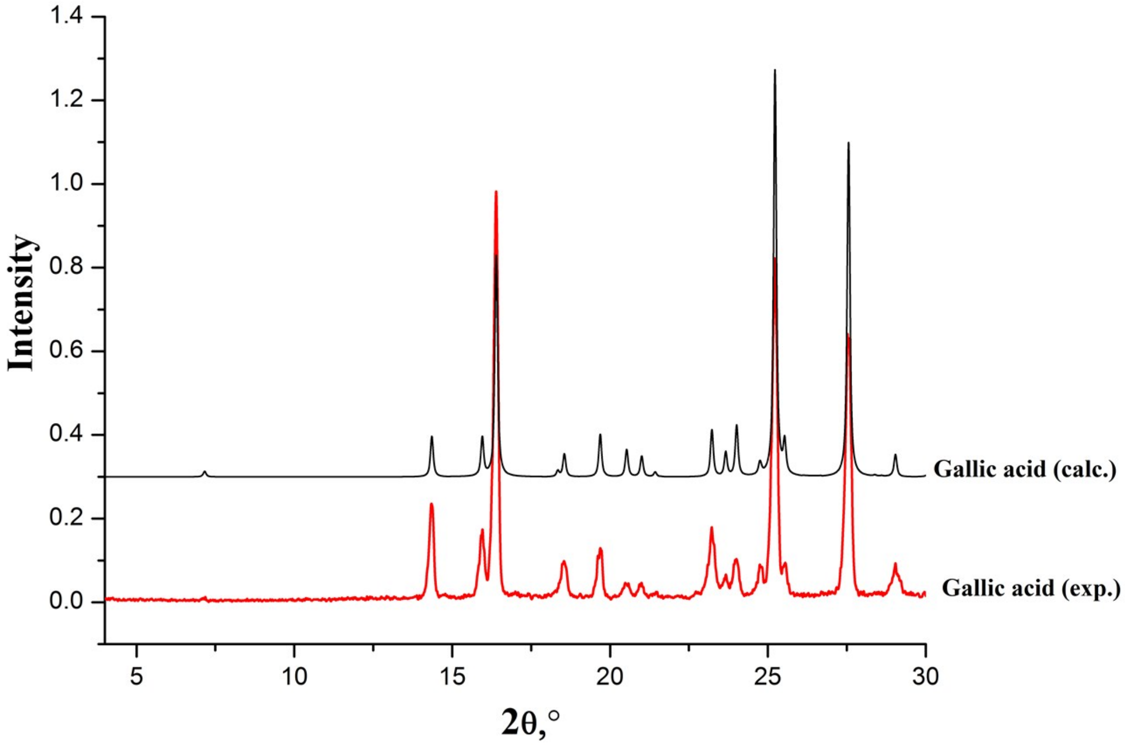

Figure S1. Experimental and calculated (IJUMEG05) PXRD patterns of gallic acid form II.

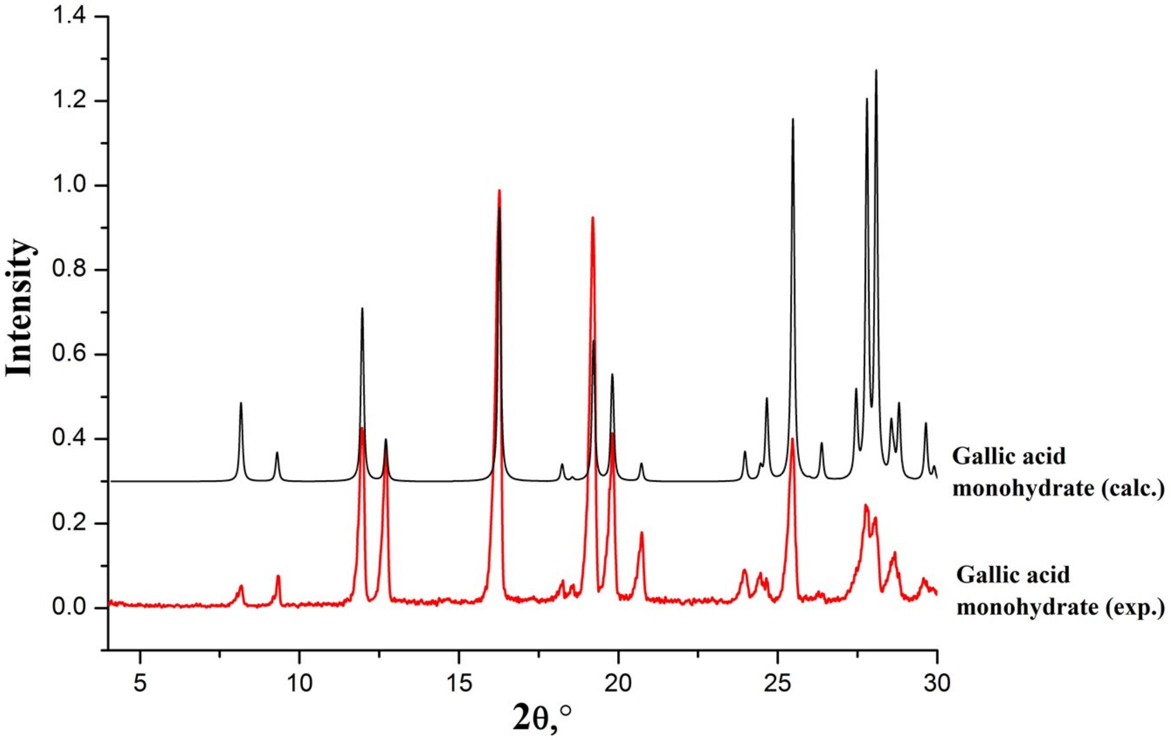

Figure S2. Experimental and calculated (IJUMEG05) PXRD patterns of gallic acid monohydrate form I.

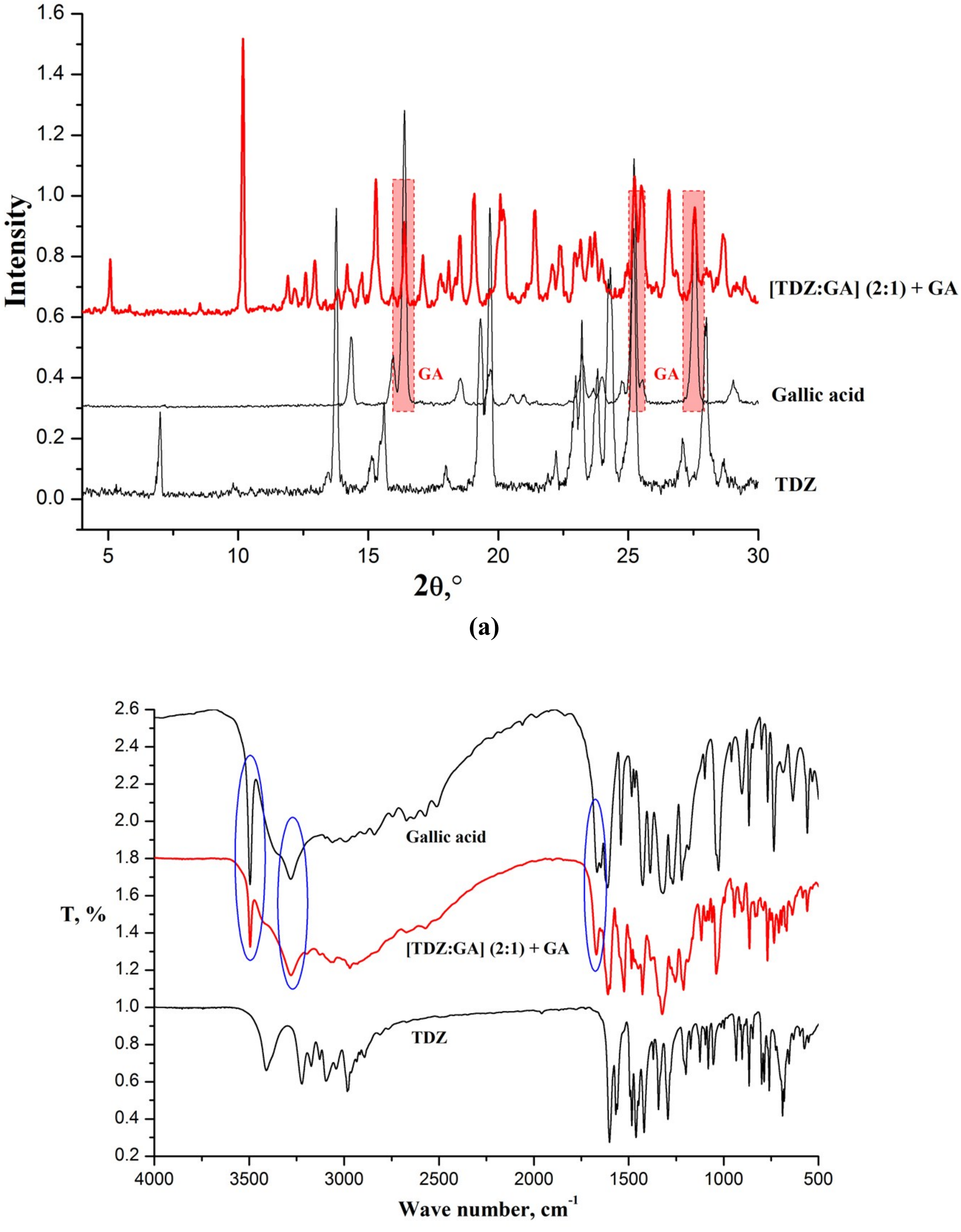

(a)

(b)

Figure S3. Experimental (a) XRPD patterns and (b) FT-IR spectra of TDZ, gallic acid and material obtained by liquid-assisted grinding of TDZ and GA in 1:1 molar ratio with acetonitrile.

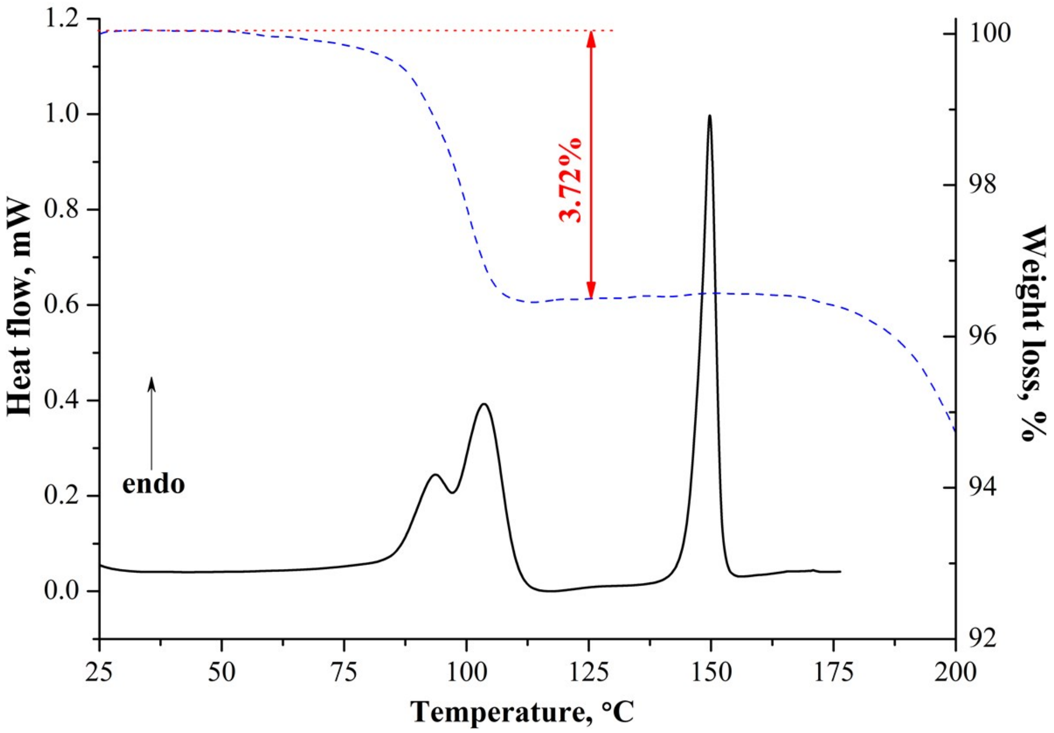

Figure S4. DSC thermogram and TG analysis of the [**TDZ**:**GA**:**H2O**] (1:1:1) cocrystal

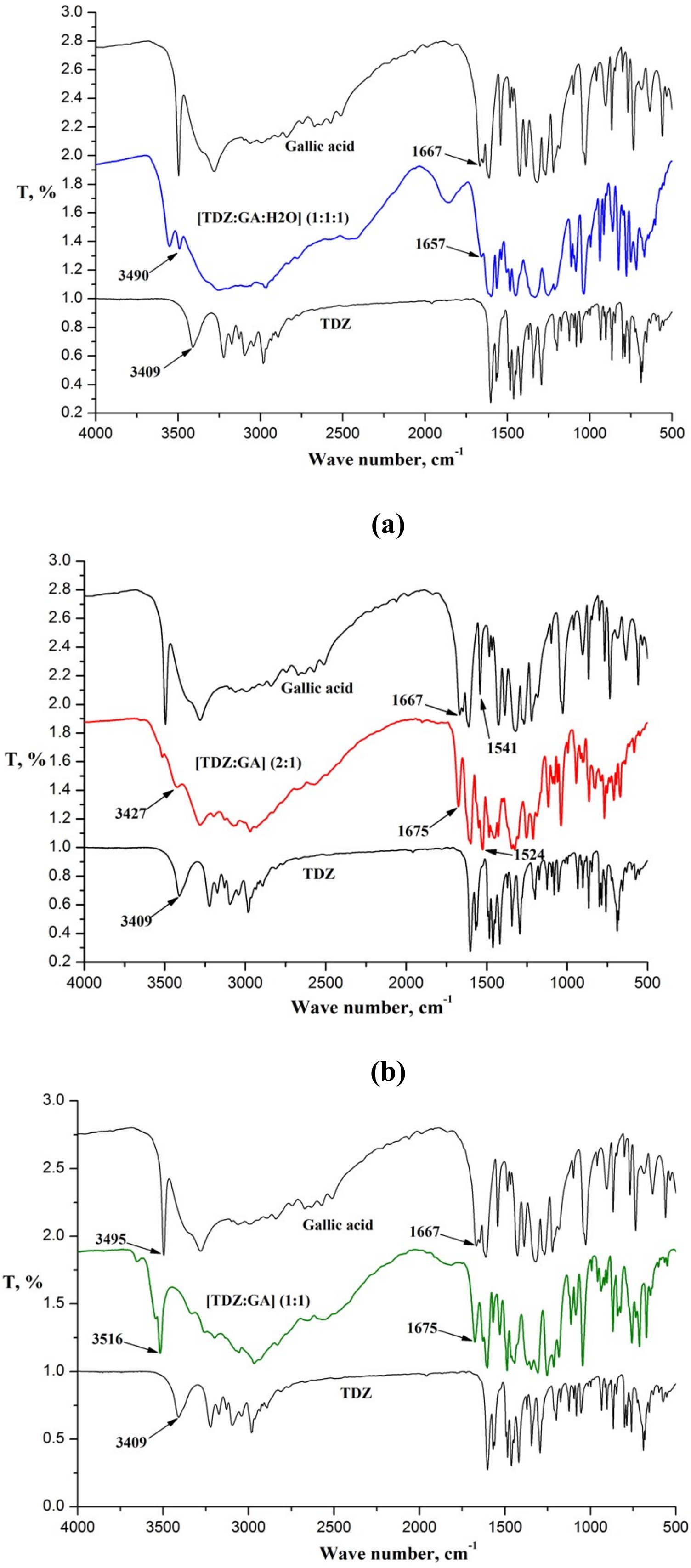

(a)

(b)

(c)

Figure S5. Experimental FT-IR spectra of TDZ, gallic acid and (a) [**TDZ**:**GA**:**H2O**] (1:1:1), (b) [**TDZ**:**GA**] (2:1), (c) [**TDZ**:**GA**] (1:1) cocrystals.

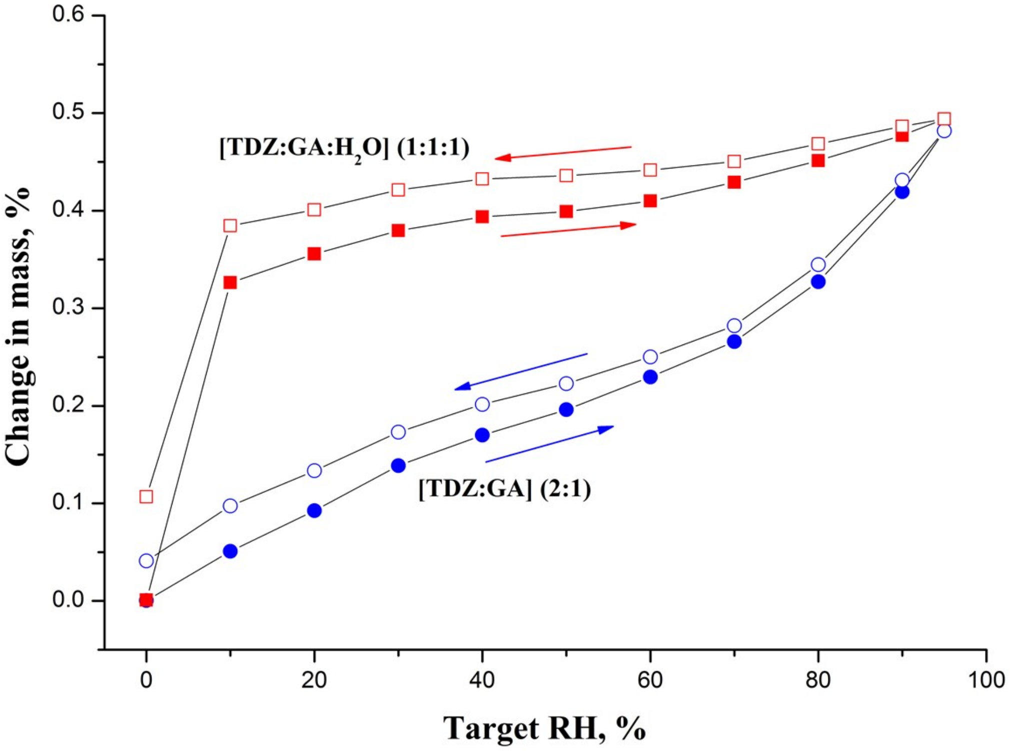

Figure S6. Water sorption (full points) and desorption (empty) curves of [**TDZ:GA**] (2:1) (blue) and [**TDZ:GA:H2O**] (1:1:1) (red) at 25°C.

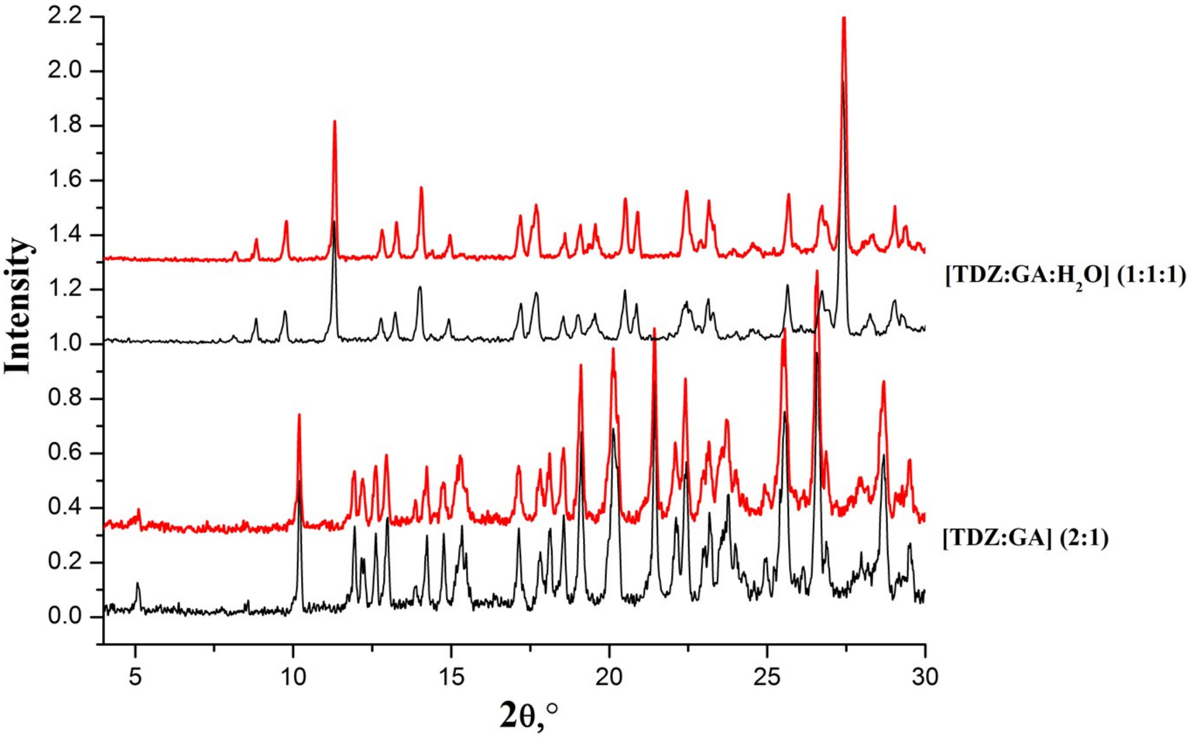

Figure S7. Experimental XRPD patterns of [**TDZ**:**GA**:**H2O**] (1:1:1) and [**TDZ**:**GA**] (2:1) before (black) and after (red) DVS studies

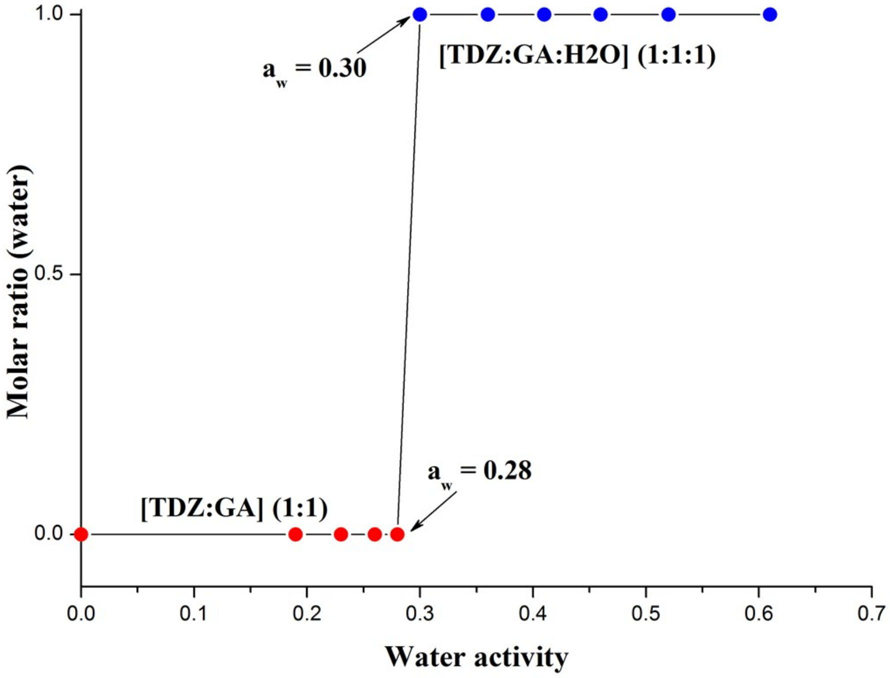

Figure S8. Phase diagram showing the dependence of the [**TDZ**:**GA**] (1:1) cocrystal stability on water activity in acetonitrile/water mixtures at 25.0 °C.

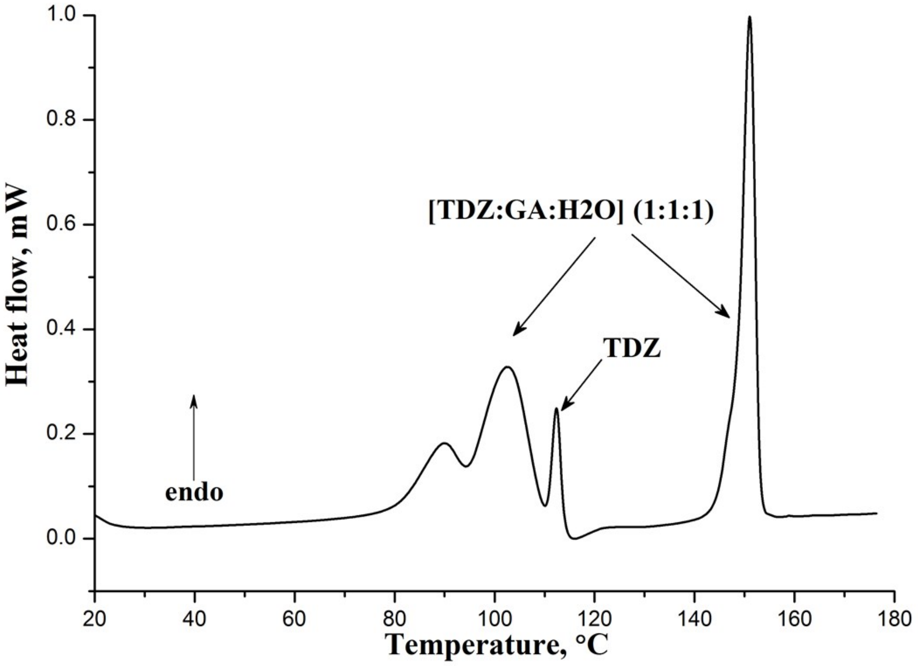

Figure S9. Example of DSC analysis of the solid phase at the eutectic point.

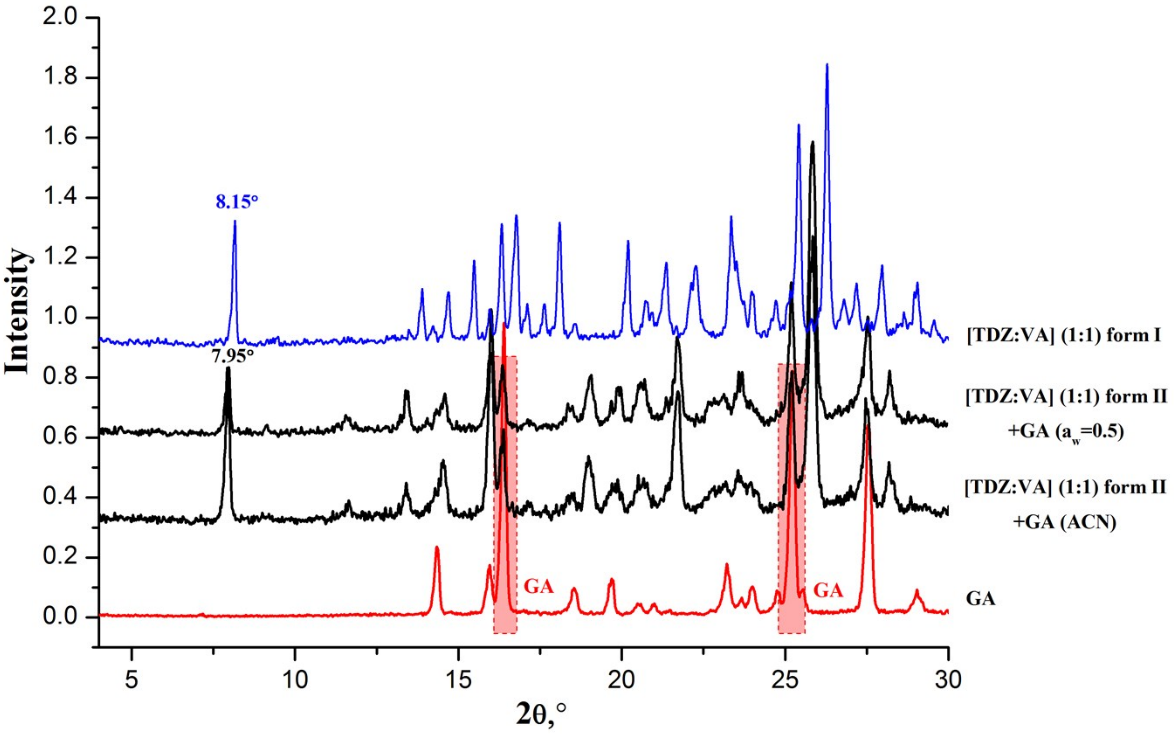

Figure S10. Experimental XRPD patterns of [**TDZ**:**VA]** (1:1) form II obtained as a result of competitive grinding reactions of TDZ, gallic acid and vanillic acid in the presence of ACN or ACN/H2O mixture with a_w = 0.5.

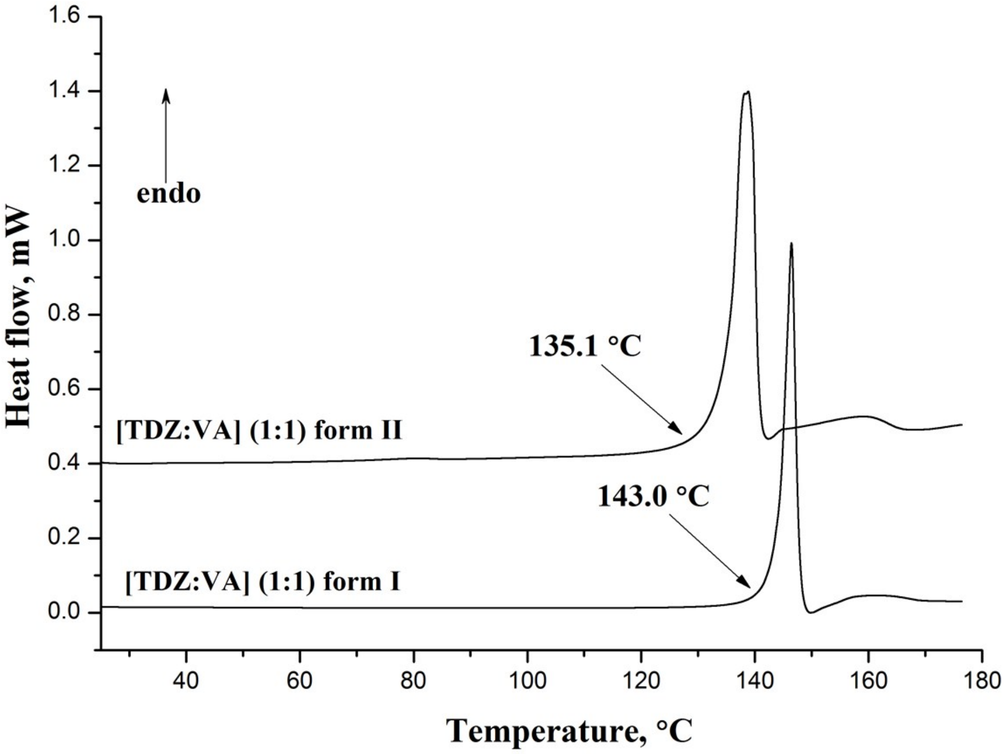

Figure S11. DSC curves of form I and form II of the [**TDZ**:**VA**] (1:1) cocrystal

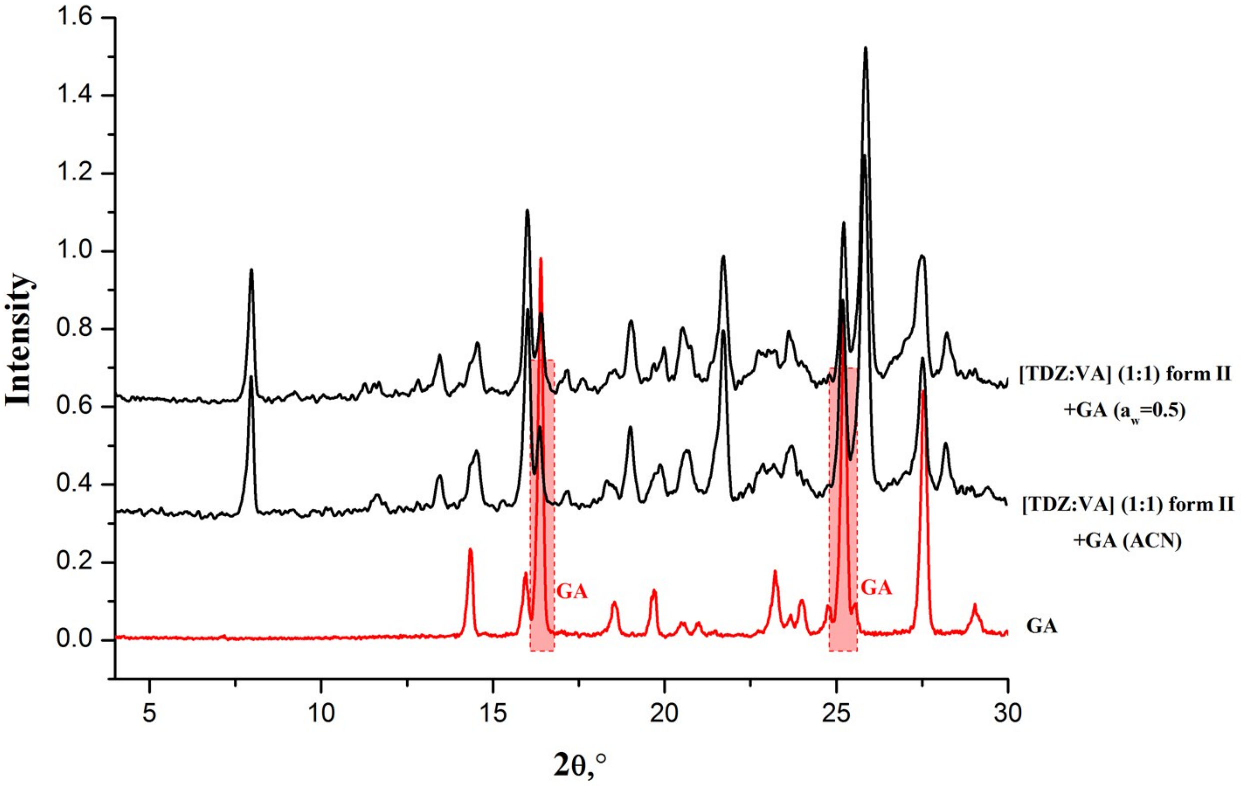

Figure S12. Experimental XRPD patterns of [**TDZ**:**VA]** (1:1) form II obtained as a result of exchange grinding reactions of **[TDZ:GA**] (2:1) with vanillic acid in the presence of ACN or ACN/H2O mixture with a_w = 0.5.

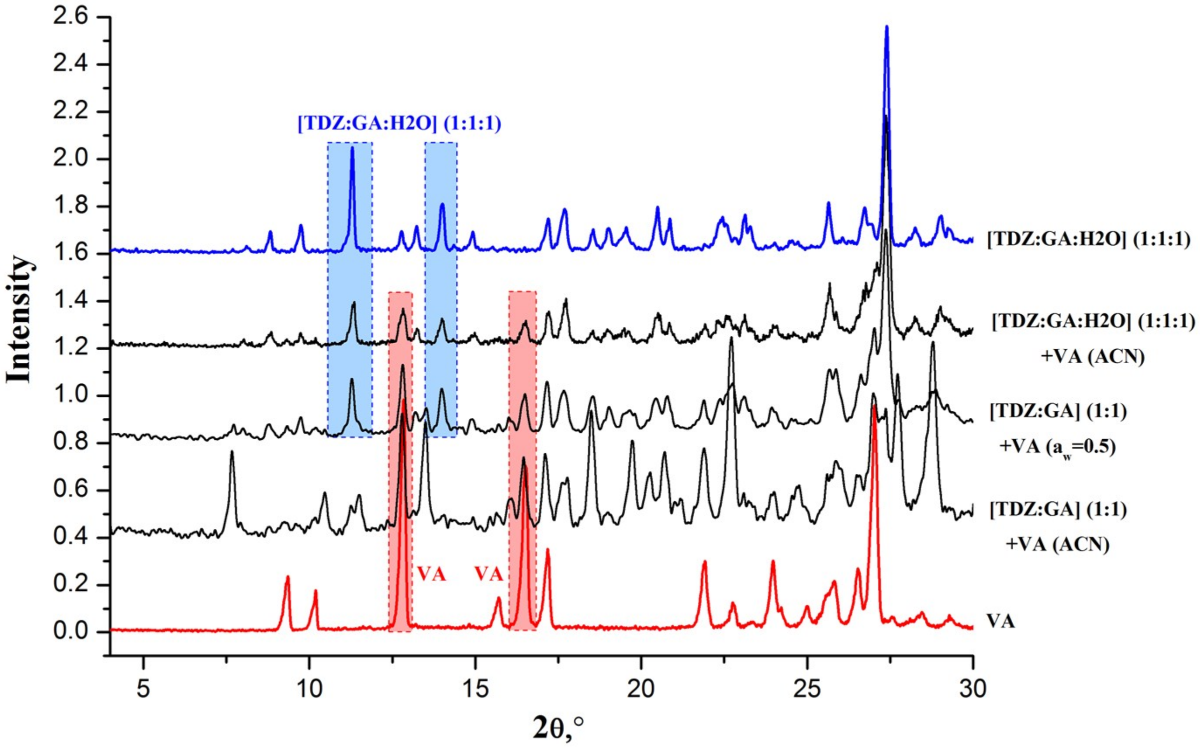

Figure S13. XRPD results of exchange grinding reactions of **[TDZ:GA]** (1:1) and [**TDZ**:**GA**:**H2O**] (1:1:1) with vanillic acid in the presence of ACN or ACN/H2O mixture with a_w = 0.5.

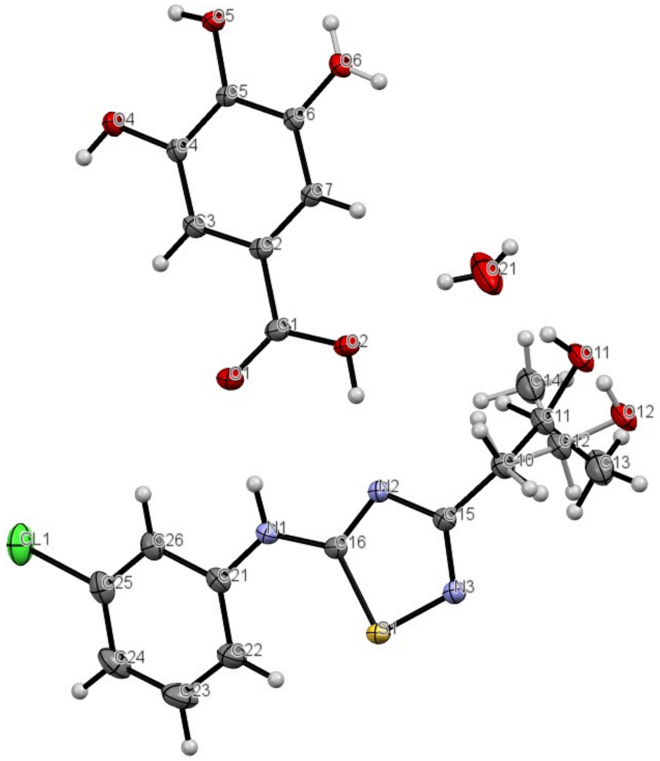

Figure S14. Molecular units in [**TDZ**:**GA**:**H2O**] (1:1:1). Displacement ellipsoids are shown at 50% probability. The higher site occupancy component in the **TDZ** molecule is shown with black bonds, and the lower one with grey bonds.

Table S1. The results of calculations of cocrystallization outcome from different predictive models for TDZ and GA or GA·H2O

	Hydrogen bond propensity calculations				Molecular complementarity	$\Delta G_f^{298}(CC)$ calc.
Molecular structure of compounds	Interactions	Propensity	Interaction type	Conclusion	Result	Result
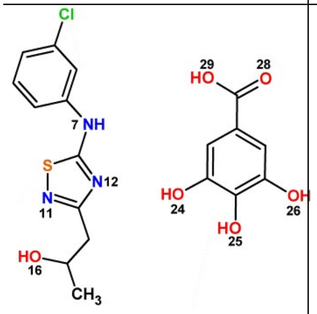	O16 – N11	0.69	TDZ-TDZ	Low probability of cocrystallization	fail	0.9 kJ/mol (Cocrystal is expected)
	O16 – N12	0.61	TDZ-TDZ			
	O29 – N11	0.56	TDZ-GA			
	O16 – O28	0.55	TDZ-GA			
	O16 – O16	0.52	TDZ-TDZ			
	O29 – N12	0.48	TDZ-GA			
	O25 – N11	0.48	TDZ-GA			
	N7 – N11	0.47	TDZ-TDZ			
	O24 – N11	0.47	TDZ-GA			
	O26 – N11	0.47	TDZ-GA			
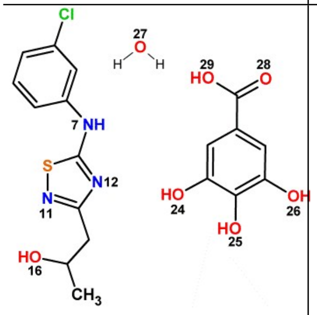	O27 – N11	0.66	TDZ-H2O	Result is inconclusive	pass	n/a
	O16 – N11	0.64	TDZ-TDZ			
	O27– O27	0.62	H2O-H2O			
	O16 – O27	0.60	TDZ-H2O			
	O27 – N12	0.58	TDZ-H2O			
	O16 – N12	0.56	TDZ-TDZ			
	O27– O29	0.56	GA-H2O			
	O27– O16	0.54	TDZ-H2O			
	O29– N11	0.52	TDZ-GA			
	O16 – O29	0.52	TDZ-GA			
	O16 – O16	0.52	TDZ-TDZ			

Table S2. Crystallographic data for the **[TDZ:GA:H2O]** (1:1:1) cocrystal

Compound reference	**[TDZ:GA:H2O]** (1:1:1)
Chemical formula	$C_{11}H_{12}ClN_3OS \cdot C_7H_6O_5 \cdot H_2O$
Formula Mass	457.88
Crystal system	Triclinic
a/ Å	9.6276(8)
b/ Å	10.1883(8)
c/ Å	11.0539(9)
α/°	90.533(1)
β/°	100.803(1)
γ/°	105.940(1)
Unit cell volume/ Å ^{3}	1021.97(14)
Temperature/K	150(2)
Space group	P-1
No. of formula units per unit cell, Z	2
Absorption coefficient, μ/mm^{-1}	0.336
No. of reflections measured	12044
No. of independent reflections	5909
R_{int}	0.0123
Final R_1 values ($I > 2\sigma(I)$)	0.0447
Final wR(F^2) values ($I > 2\sigma(I)$)	0.1083
Final R_1 values (all data)	0.0474
Final wR(F^2) values (all data)	0.1097
Goodness of fit on F^2	1.182
Largest diff. peak & hole, e·Å^{-3}	0.483 / -0.529

Table S3. Characteristics of the intermolecular (noncovalent) interactions in around water molecule in the crystals of [TDZ:GA:H2O] (1:1:1) build of TDZ conformation I and TDZ conformation II calculated by the solid-state DFT method coupled with the QTAIMC analysis of the periodic wave-function*

Interaction	D(D···A)/ Å (D(H···A)/ Å)	ρ_b/ a.u.	$\nabla^2\rho_b$/ a.u.	G_b/ a.u.	E_{int}/ kJ·mol^{-1}
TDZ conformation I					
O11-H11···O21	2.800 (1.823)	0.033	0.098	0.024	**27.5**
O21-H20···O1	2.855 (1.883)	0.028	0.081	0.020	**22.7**
O6-H61···O21	2.872 (1.978)	0.025	0.070	0.018	**20.6**
O21-H21···O5	2.876 (2.115)	0.019	0.058	0.015	**16.7**
C10-H10B···O21	3.774 (2.709)	0.007	0.026	0.005	**5.8**
C10-H10A···O21	3.704 (2.739)	0.006	0.023	0.005	**5.3**
TDZ conformation II					
O21-H20···O1	2.855 (1.892)	0.027	0.081	0.020	**22.9**
O6-H61···O21	2.872 (1.938)	0.027	0.072	0.019	**21.5**
O21-H21···O5	2.876 (2.252)	0.015	0.053	0.013	**14.3**
C10-H10D···O21	3.597 (2.607)	0.007	0.028	0.006	**6.3**
C14-H14B···O21	3.763 (2.785)	0.005	0.019	0.004	**4.3**

*The D···A and H···A distances, *D*(X···A) and *D*(H···A), where D, A = O, and C; the electron density ρ_b , the Laplacian of the electron density $\nabla^2\rho_b$ and local electronic kinetic energy density G_b at the bond critical point; the energy of the intermolecular noncovalent interaction E_{int}.

Table S4. Coformers, calculated values of Gibbs energy of cocrystal formation, predicted outcomes of cocrystallization along with experimental results.

Coformer	TDZ:coformer mol. ratio	$\Delta G_f^{298}(CC)$ calc, [kJ·mol^{-1}]	Predicted outcome	Experimental result
2-Hydroxybenzamide	1:1	12.2	Cocrystal is not expected	no cocrystal
4-Aminobenzoic acid	1:1	6.8	Cocrystal is not expected	no cocrystal
4-Hydroxybenzoic acid	1:1	8.5	Cocrystal is not expected	no cocrystal
4-Hydroxybenzamide	1:1, 1:2	-0.8, 3.6	Cocrystal is expected	no cocrystal
Benzamide	1:1	22.7	Cocrystal is not expected	no cocrystal
Benzoic Acid	1:1	6.4	Cocrystal is not expected	no cocrystal
Caffeine (form I)	1:1	8.3	Cocrystal is not expected	no cocrystal
Malonic acid	1:1	46.7	Cocrystal is not expected	no cocrystal
Nicotinamide	1:1	21.9	Cocrystal is not expected	no cocrystal
Pimelic Acid	1:1, 2:1	-21.1, -25.1	Cocrystal is expected	no cocrystal
Pyrazinamide	1:1	8.9	Cocrystal is not expected	no cocrystal
2-Hydroxybenzoic acid	1:1	2.0	Cocrystal is expected	no cocrystal
Succinic acid	1:1	5.6	Cocrystal is not expected	no cocrystal
1,2-phenylenediamine	1:1	-0.3	Cocrystal is expected	
Flufenamic Acid	1:1, 2:1	-1.7, -5.3	Cocrystal is expected	
Fumaric Acid	1:1	-1.5	Cocrystal is expected	
Phenazine	1:1, 2:1	4.1, 2.6	Cocrystal is expected	

References

1. G. Sheldrick, *Journal*, 1997.
2. G. Sheldrick, *Acta Crystallographica Section A*, 2008, **64**, 112-122.
3. R. Dovesi, R. Orlando, A. Erba, C. M. Zicovich-Wilson, B. Civalleri, S. Casassa, L. Maschio, M. Ferrabone, M. De La Pierre, P. D'Arco, Y. Noël, M. Causà, M. Rérat and B. Kirtman, *International Journal of Quantum Chemistry*, 2014, **114**, 1287-1317.
4. S. Grimme, *Journal of Computational Chemistry*, 2006, **27**, 1787-1799.